THE JOURNAL OF PHYSICAL CHEMISTRY A

 VOLUME 112, NUMBER 16, APRIL 24, 2008

ARTICLES

Ionization of Imidazole in the Gas Phase, Microhydrated Environments, and in Aqueous Solution

Barbara Jagoda-Cwiklik,[†,‡] Petr Slavíček,[§] Lukasz Cwiklik,[†] Dirk Nolting,[||] Bernd Winter,[||] and Pavel Jungwirth*[,†]

Institute of Organic Chemistry and Biochemistry, Academy of Sciences of the Czech Republic, and Center for Complex Molecular Systems and Biomolecules, Flemingovo nám. 2, 16610 Prague 6, Czech Republic, Fritz Haber Institute for Molecular Dynamics, Hebrew University, Jerusalem 90904, Israel, Department of Physical Chemistry, Institute of Chemical Technology, Technická 5, Prague 6, Czech Republic, and Max-Born-Institut für Nichtlineare Optik und Kurzzeitspektroskopie, Max-Born-Strasse 2A, D-12489 Berlin, Germany

Received: December 5, 2007; In Final Form: January 14, 2008

Hydration of neutral and cationic imidazole is studied by means of ab initio and molecular dynamics calculations, and by photoelectron spectroscopy of the neutral species in a liquid microjet. The calculations show the importance of long range solvent polarization and of the difference between the structure of water molecules in the first shell around the neutral vs cationic species for determining vertical and adiabatic ionization potentials. The vertical ionization potential of neutral imidazole of 8.06 eV calculated using a nonequilibrium polarizable continuum model agrees well with the value of 8.26 eV obtained experimentally for an aqueous solution at pH 10.6.

1. Introduction

Imidazole ($C_3N_2H_4$) is a heterocyclic aromatic compound that is the building block of many technologically and biologically relevant molecules. Its substituents are often used as cations in ionic liquids.[1] The imidazole ring also forms the titratable part of the side chain of the amino acid histidine, which may be either neutral or protonated within proteins at pH 7. Imidazole can thus be regarded as a suitable model system for studying pH-dependent processes at surfaces of hydrated proteins.

In the present combined computational and experimental study, photoelectron spectroscopy (PES) is applied to directly measure the lowest vertical electron binding energy of neutral imidazole in aqueous solution. PES studies of the electronic structure of aqueous solutions are still scarce because of the high vapor pressure, which has hampered the measurement of kinetic energies of the photoelectrons. Only with the recent development of the liquid microjet technique has PE spectroscopy from aqueous solutions under vacuum conditions become possible.[2] In direct connection to the PES experiment, we aimed to calculate ionization energies of imidazole in the gas phase and in the solution. The vertical ionization potential (VIP) was evaluated as the difference between the energy of the optimized neutral structure and that of the corresponding cationic system at the neutral geometry. This calculated value can be directly compared with the measured maximum of the corresponding photoelectron peak. The adiabatic ionization potential (AIP) was calculated as the difference between the energy of the optimized neutral molecule and the energy of the optimized cation. Adiabatic ionization potential thus additionally reflects the nuclear relaxation taking place after the electron removal. Given

* Corresponding author. E-mail: pavel.jungwirth@uochb.cas.cz.
[†] Academy of Sciences of the Czech Republic.
[‡] Hebrew University.
[§] Institute of Chemical Technology.
[||] Max-Born-Institut für Nichtlineare Optik und Kurzzeitspektroskopie.

10.1021/jp711476g CCC: $40.75
Published on Web 03/12/2008

that there is a nonzero Franck−Condon overlap, AIP correlates with the low energy onset of the experimental photoelectron peak.

A direct quantum chemical calculation of the ionization potentials, as employed for isolated molecules, cannot be utilized for solutes immersed in water or other solvents since it is computationally prohibitive. Therefore, we have adopted three alternative approaches: (i) microsolvation of the solute, (ii) a mixed quantum chemical/molecular dynamics approach, and (iii) a continuum solvent model. Within the first approach, a supermolecule composed of the solute and a small number of solvating molecules is studied utilizing *ab initio* quantum chemical methods. Even though molecular clusters ultimately converge to extended systems, this convergence is usually prohibitively slow, which prevents gaining quantitative information on bulk behavior from cluster calculations. Moreover, finite temperature effects are missing in this approach. To overcome this limitation, we have studied within the second approach imidazole with a large number of water molecules represented exclusively by their charges with geometries sampled using a classical molecular dynamics (MD) bulk simulation. In this way, finite temperature effects, as well as long-range nuclear polarization of water by neutral imidazole is accounted for; however, contributions from electronic polarization are not included in the calculation. In the third approach, we used a nonequilibrium version of the polarizable continuum model (PCM)[3−5] to account for all the nonspecific solvation effects. Within this approach, we solvated either bare imidazole or added a small number (up to five) explicit water molecules, and evaluated the corresponding vertical ionization potentials.

It is important to note that ionization involves an instantaneous change of charge state of the solute molecule and is accompanied by fast electronic response of the solvent molecules, similarly to the cases of electronic excitation and electron transfer.[6] Within the PCM model, this situation can be described using a time-dependent polarization vector $P(t)$.[4,7−9] $P(t)$ can be partitioned into a P_{fast} component corresponding to the polarization of the electronic cloud, and a P_{slow} component corresponding to nuclear degrees of freedom (orientational polarization). On the time scale of the sudden change of electronic distribution of the solute upon ionization or electronic excitation, the solvent nuclear structure cannot rearrange. Within the Franck−Condon approximation, the electronic part of polarization can thus be considered to be infinitely fast, while the orientational part relaxes on the time scale of picoseconds to nanoseconds, depending on the particular solvent. These considerations lead to a concept of nonequilibrium continuum solvation. Here, the solvent reaction field is optimized for the molecule in the ground state, and this field is then used for calculating the energy of the ionized or electronically excited species. This concept of nonequilibrium solvation has been successfully applied mostly in the context of electronic absorption spectra, but it has also been used to study processes following detachment of the electron.[10] Here, we find it very well suited for interpreting the PE spectra, where each peak corresponds to the most probable excitation energy that vertically ejects an electron from a bound state into the vacuum with zero kinetic energy.

In this paper we present valence-band photoemission data from imidazole aqueous solution at basic pH. The experimental vertical ionization potential is compared with values obtained from combined *ab initio* and MD calculations. The paper is organized as follows. Section 2 presents experimental and computational details. The results of PES measurements and combined *ab initio* and molecular dynamics calculations are shown in Section 3. A discussion of the results and conclusions are presented in Section 4.

2. Experimental Method

Photoemission studies of aqueous solutions of imidazole were performed at the U41 PGM undulator beamline of the synchrotron radiation facility BESSY (Berlin). PE spectra were collected from a 15 μm liquid microjet traveling at a velocity of 120 m/s with a temperature of 4 °C. In the present study we have used a photon energy of 200 eV. Details of the experimental setup and a discussion concerning the application of photoelectron spectroscopy to highly volatile aqueous solutions have been reported previously.[2] Briefly, excitation is carried out with the synchrotron light polarization vector parallel to the flow of the liquid microjet, while the mean electron detection angle is normal to the polarization vector. Photoelectrons are collected through an orifice 200 μm in diameter, which acts as a conductance-limiting aperture to differentially pump the main chamber housing the liquid microjet (operating at 10^{-5} mbar) from the hemispherical kinetic energy analyzer (operating at 10^{-9} mbar). Energy resolution of the beamline was better than 200 meV at the incident photon energy used here. The resolution of the hemispherical kinetic energy analyzer is constant with kinetic energy (200 meV at a constant analyzer energy of 20 eV). Typical signal count rates were 10^3-10^4 s^{-1}. The small focal size (23×12 μm^2) of the incident photon beam at the U41 PGM beamline allows for matching spatial overlap with the liquid microjet, which limits the contribution of gas-phase components in the collected photoemission spectra to less than 5% for liquid water. Electron kinetic energies (eKE) are calibrated on the basis of the $1b_1$ binding energy (BE) of liquid water.[11]

Highly demineralized water was used for preparing the 2 m imidazole aqueous solutions. Imidazole was purchased from Merck and was used without further purification. A room-temperature pH value of 10.6 was determined with an accuracy of $\pm$ 0.1 pH units using a pH meter (766, Knick) with a single-rod measuring cell (SE 100, Knick). At this pH, 99% of all imidazole molecules are neutral.

2.1. Computational Methods. In order to obtain reliable values of the ionization energy of imidazole, we have to consider both basis set and correlation energy effects. The aug-cc-pVDZ basis provides an acceptable compromise between accuracy and computational feasibility. Concerning correlation energy, density functional theory (DFT) and Møller-Plesset (MP2) perturbation calculations again represent a reasonable compromise between accuracy and computational cost, allowing for calculations with at least the nearest solvent molecules treated quantum mechanically. For open-shell systems, such as the imidazole radical cation, the unrestricted wave function can be contaminated by higher spin states. This problem is less severe for DFT-based methods than for MP2, but DFT methods can suffer from other possible artifacts, such as the spurious charge delocalization due to the self-interaction error. There is an option to project out the higher spin components in MP2 by a procedure suggested by Schlegel (the PMP2 method).[12] We have thus utilized the following protocol. Neutral imidazole geometry was optimized at the MP2/aug-cc-pVDZ level, while the imidazole radical cation was optimized at the UMP2 level with the PMP2 correction applied for the optimal geometry. Note that this procedure is meaningful only if the spin contamination of the unrestricted wave function is within reasonable margins. In all our calculations, the expectation value of S^2 was always below

0.85. It has been previously shown that the UMP2/PMP2 protocol leads to a good description of ionization energies.[13] Furthermore, we have tested our results against the coupled clusters method CCSD(T), which includes a larger portion of the correlation energy, and by multireference based methods (CAS-SCF, CASPT2 and MRCI), accounting for non-dynamic correlations. Here, we have chosen an active space consisting of six electrons placed in six frontier orbitals.

For each of the neutral imidazole$(H_2O)_n$ clusters, geometry optimization was performed at the MP2/aug-cc-pVDZ level of theory. For clusters with up to two water molecules, we started from various chemically plausible structures employing no symmetry constraints. Clusters with three to five water molecules already possess an exceedingly large number of degrees of freedom for such a procedure. Therefore, we chose initial structures for geometry optimization from *ab initio* molecular dynamics trajectories. These simulations were carried out using the CP2K/Quickstep code[14] employing a DFT approach with the BLYP functional and the double-ζ DZVP basis set. After each MP2 optimization starting from DFT structures, we performed frequency analysis to verify that optimized structures correspond to minima on the potential energy surface. Vertical ionization potentials were then calculated with the PMP2 method as described above. Moreover, in the case of $n = 0-2$, we also optimized cationic structures in order to calculate adiabatic transitions. For clusters that contained less than three water molecules, we additionally evaluated VIPs at the CCSD(T), CASPT2, and MRCI levels of theory.

In order to mimic imidazole behavior in bulk water, we ran classical MD simulations employing the Amber8 simulation package.[15] We used the SPC force-field for water molecules, while the force-field for imidazole was derived using the Antechamber software employing the Generalized Amber Force Field (GAFF) parametrization.[16,17] We simulated a system consisting of a single imidazole molecule in bulk water with 800 H_2O molecules in the unit cell. Periodic boundary conditions were applied with a simulation box of $25 \times 25 \times 25$ Å^3. Simulations were performed in the canonical (NVT) ensemble at $T = 300$ K. After equilibration, we took 99 snapshots from the nanosecond trajectory for further calculations. For these we removed all water molecules at a distance larger than 10 Å from the center of mass of the imidazole molecule (in order to carve a spherical solvent environment out of the cubic simulation box). We then carried out the following *ab initio* calculations: MP2/aug-cc-pVDZ single-point energy calculations for imidazole, and PMP2/aug-cc-pVDZ for the corresponding imidazole cation, with all water molecules represented as SPC fractional charges located at atomic positions.

As a next step, we chose at random 10 configurations from the above set and performed single-point energy calculations for neutral imidazole and imidazole cation with the first solvation shell of water molecules included explicitly in the ab initio calculation, while the remaining water molecules were represented as point charges. The explicit water molecules resided within the radius of 4.5 Å from the center of mass of imidazole, and their average number was nine. Additionally, we performed *ab initio* molecular dynamics simulations with CP2K/Quickstep for imidazole in bulk water, with 31 water molecules in the unit cell. These calculations were performed with the BLYP functional and DZVP basis set in the NVT ensemble at $T = 300$ K. We took from the trajectory three snapshots containing the 31 solvent molecules in the unit cell, and we carried out single-point energy calculations as above, i.e., either with water molecules as point charges or with the first solvent shell taken explicitly.

TABLE 1: Comparison of MP2/aug-cc-pvdz (MP2/aug-cc-pvtz) and Experimental Ionization Potential of Halide Anions in the Gas Phase

anion	MP2/aug-cc-pvdz (aug-cc-pvtz)	experimental ionization potential in the gas phase[a]
F^-	3.51 (3.59)	3.40
Cl^-	3.52 (3.58)	3.61
Br^-	3.37 (3.44)	3.36
I^-	3.15 (3.21)	3.06

[a] Reference 19.

TABLE 2: Comparison of Equilibrium and Nonequilibrium PCM MP2/aug-cc-pvdz (MP2/aug-cc-pvtz) Results with Experimental Vertical Ionization Potential of Halide Anions in Water

anion	equilibrium PCM MP2/aug-cc-pvdz (aug-cc-pvtz)	nonequilibrium PCM MP2/aug-cc-pvdz (aug-cc-pvtz)	experimental vertical ionization potential in water[a]
F^-	7.36 (7.47)	9.63 (9.79)	9.8 (estimated)
Cl^-	6.63 (6.71)	8.55 (8.63)	9.6
Br^-	6.24 (6.34)	8.05 (8.14)	8.8
I^-	5.71 (5.85)	7.40 (7.48)	7.7

[a] Reference 20.

As a final alternative, the effect of bulk water on the ionization potential was modeled using the polarizable continuum model (PCM).[4−5,7] VIP and AIP were calculated at the PMP2/aug-cc-pVDZ level using geometries of imidazole and imidazole cation, both optimized in the gas phase. To calculate AIP, the reaction field was optimized both for the neutral and cationic state. To calculate VIP, we first optimized the reaction field for the neutral molecule. In a subsequent step, we employed the nonequilibrium solvation protocol as implemented in Gaussian 03.[8,9,18] Within this approach, the fast electronic component of the polarization was included, while the nuclear orientational polarization was not, which corresponds to vertical ionization.

Since we are not aware of any benchmarking of nonequilibrium PCM, we performed test calculations for ionization of the series of halide anions, for which experimental values are well-established both in the gas phase and in water (except maybe for aqueous fluoride). First, Table 1 presents gas-phase ionization potentials of F^-, Cl^-, Br^-, and I^- at the MP2 level with aug-cc-pvdz and aug-cc-pvtz basis sets (employing a pseudopotential for iodide, i.e., the aug-cc-pvdz-PP or aug-cc-pvtz-PP basis). These results show that the MP2 method is able to reproduce, already with the smaller basis set, experimental[19] gas-phase ionization potentials within 0.2 eV. Table 2 then compares results from equilibrium vs nonequilibrium PCM to experimental[20] vertical ionization potentials in water. As already shown in our previous studies,[20,21] equilibrium PCM strongly underestimates the experimental values, since this method rather corresponds to adiabatic ionization. Note the somewhat different values of ionization potentials obtained using equilibrium PCM in this study compared to the previous one.[20] This difference (which is small for heavier halides but relatively large for fluoride) is primarily due to reparametrization of the sizes of dielectric cavities done in the newer version of the Gaussian program.[8,9,18] The most important result is, however, that employing nonequilibrium PCM (Table 2) dramatically reduces the gap between calculations and experiment, from more than 3 eV to 1 eV (chloride) or even significantly less (other halides). After this successful benchmarking on halides, below we apply

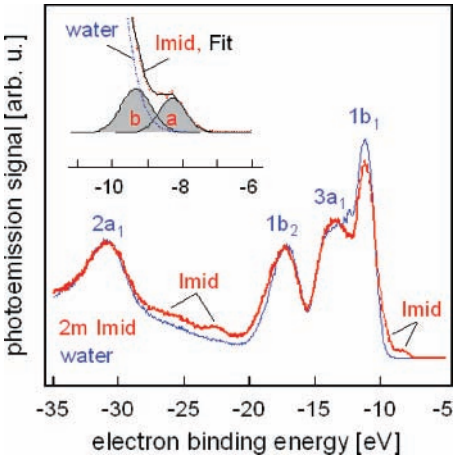

Figure 1. Valence photoelectron spectra of 2 m imidazole aqueous solution (pH 10.6) and of pure liquid water measured at 200 eV photon energy. Intensities are normalized to the height of the $2a_1$ emission peak of liquid water. The inset figure is an enlargement of the spectral region of photoemission onset, again contrasting the solution and liquid water. The black curve is the fit to the experimental solution spectrum, using three Gaussians (as explained in the text). Peak **a**, with maximum at −8.26 eV electron binding energy, represents photodetachment from the HOMO of neutral imidazole(aq).

nonequilibrium PCM to a challenging problem of ionization of a nonspherical molecular species.

Polarizable continuum models cannot describe specific solvation effects. However, most of these specific solvation effects can usually be traced to the influence of water molecules in the first solvent shell. To explore this possibility, we also employed a hybrid model, in which clusters with a small number of explicitly treated solvating water molecules are immersed in the polarizable continuum. The explicit treatment of the clusters was again performed at the MP2/PMP2 level. The ab initio calculations were done using the Gaussian 03 suite of programs,[18] except for test multireference calculations performed using the MOLPRO package.[22]

3. Results

3.1. Photoemission from Imidazole Aqueous Solution. Figure 1 contrasts the valence PE spectrum of 2 m aqueous imidazole (red) with that of pure liquid water (blue). The pH of the as-prepared (no base added) solution was 10.6, and hence virtually all (>99%) imidazole molecules are neutral (deprotonated). Spectra were collected with an incident photon energy of 200 eV. Intensities are normalized to the $2a_1$ peak of liquid water, and electron binding energies (BE) are with respect to the $1b_1$ orbital of liquid water.[23] Spectral photoemission contributions from the imidazole(aq) molecule can be identified by the energies at which the intensities for the solution are larger than that for pure water. Intensities in the −30 to −18 eV BE range arise from the carbon and nitrogen atoms of the imidazole ring. A detailed assignment in this spectral region was not attempted here. Our interest is rather in the determination of the lowest-binding energy peak of aqueous neutral imidazole, associated with the (lowest) vertical ionization potential (VIP). Fortunately, this energy can be easily determined from the PE spectrum because the VIP of neutral imidazole(aq) is considerably lower than the onset energy for ionizing liquid water (in a one-photon process), the former giving rise to the small foot-like spectral feature at an energy between 8 and 9 eV. Note that, unlike VIP, which is associated with the PE peak maximum, the adiabatic ionization potential is more difficult to determine from the spectrum. If there is a lack of Franck−Condon overlap between the initial and final states, AIP does not coincide with the onset of the PE peak, which seems to be the case here (see comparison with calculated results in Section 3.4).

In order to determine the exact value of the VIP of deprotonated imidazole(aq), we have fitted the near-threshold spectral region, as shown in the inset of Figure 1. Here, three Gaussians were assumed: one for the water $1b_1$ emission peak (only the high-energy tail is shown in the figure; dotted blue), one for a feature labeled as **b**, and the third for electron emission from the imidazole(aq) highest occupied molecular orbital (HOMO), which is labeled as **a**. The Gaussian curve for the water $1b_1$ PE peak can be accurately determined from the pure water spectrum, and the peak positions and widths of the two remaining Gaussians are free fitting parameters. For the feature **a**, we obtained a binding energy of −8.26 eV and a peak width of 0.95 eV. Note that both photoemission peaks **a** and **b** are absent in acidic solution (measured at pH 2.5, in which case more than 99.99% of the imidazole molecules are protonated). Therefore, we attribute the feature **b**, peaking at −9.33 eV (i.e., 1.07 eV below peak **a**), to photoemission from the HOMO-1 orbital of neutral imidazole. This interpretation is supported by an auxiliary CASPT2 calculation, which places the first excited-state of the cation 1.2 eV above its ground state.

3.2. Computational Results. *3.2.1. Imidazole in the Gas Phase*. The MP2/ aug-cc-pVDZ optimized structure of the bare neutral imidazole is planar with C_s symmetry (Figure 2a), consistent with a previous theoretical study.[24] The geometry of the optimized imidazole cation (Figure 2d) is almost the same as that for the neutral species, both being planar. H−O bonds have practically the same length, and the lengths of both C−N and C−C bonds, as well as the values of all angles, change less than 4% upon moving from neutral to cationic imidazole. In order to choose an appropriate *ab initio* method for vertical and adiabatic ionization potential calculations, we performed a series of test calculations employing various levels of theory, as described in detail in section 2.2. Calculated values of vertical and adiabatic ionization potentials of imidazole in the gas phase are presented in Table 3. Post-Hartree−Fock methods are consistent with the experimental values.[25] Experimental adiabatic ionization potential is 8.67 eV, while the calculated one at the PMP2 level is 8.78 eV (taking zero point energy into account, AIP rises by only 0.1% and amounts to 8.79 eV). Note that a good agreement between different methods that account for correlation effects is achieved, and already description at the MP2 level is satisfactory. Also note that multireference effects are of minor importance in this case, leading to slightly lower values of both VIP and AIP. This is similar to the situation for structurally close nucleic acid bases.[26]

3.2.2. Imidazole Microhydration. The first water molecule binds to the unprotonated nitrogen (Figure 2b). The N−H hydrogen-bond (H-bond) distance is 1.93 Å, and the binding energy is 7.5 kcal/mol. We also found a secondary minimum, with water bound to the hydrogen at the protonated nitrogen, which lies only 1.25 kcal/mol above the global minimum. The O−H hydrogen bond distance in this case is also 1.93 Å. Interestingly, the geometry of this cluster is very similar to that of an optimized imidazole cation with one water molecule (shown in Figure 2e).

The lowest energy structure of the neutral imidazole$(H_2O)_2$ cluster is depicted in Figure 2c. The first water molecule is H-bonded to a nitrogen atom, while the second one is involved in a water−water H-bond and is also weakly bound to the acidic hydrogen of imidazole. The H-bond length with the nitrogen

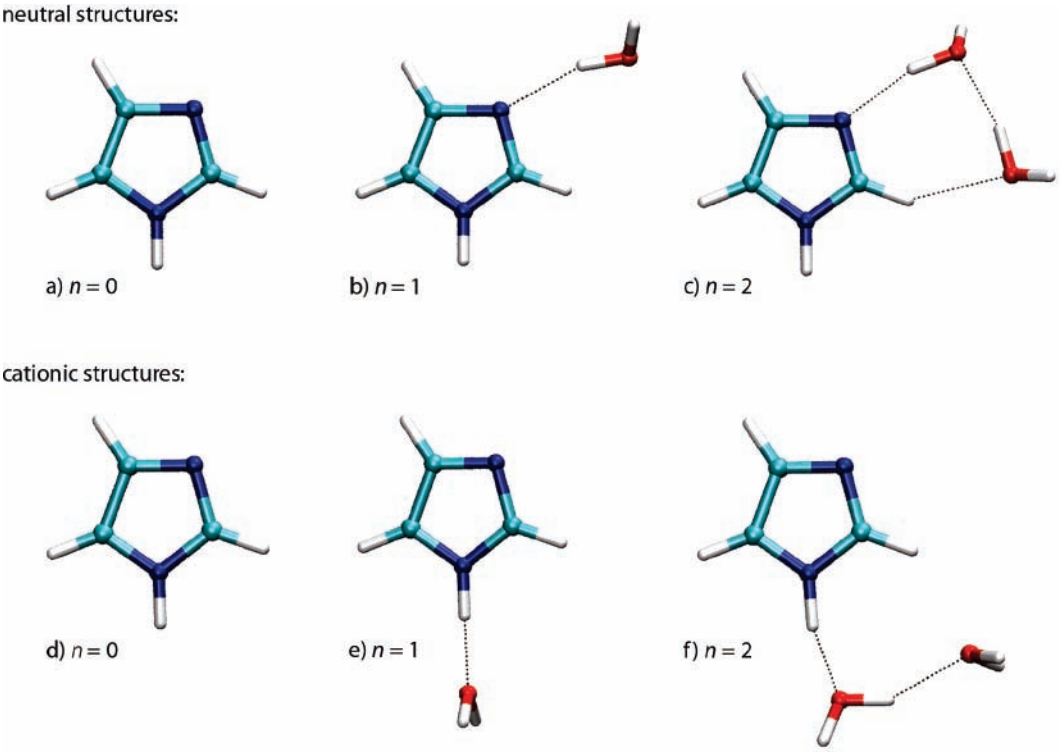

Figure 2. Structures of neutral and cationic structure of imidazole$(H_2O)_n$ clusters for $n = 0-2$.

TABLE 3: Adiabatic (AIP) and Vertical (VIP) Ionization Potentials (in eV) of Neutral Imidazole Molecule Calculated at Different Levels of Theory

method	VIP [eV]	AIP [eV]
UHF/6-31+g*	7.42	7.24
PUHF/6-31+g*	7.14	6.94
ROHF/6-31+g*	7.68	7.53
B3LYP/6-31+g*	8.88	8.71
UMP2/aug-cc-pVDZ	9.19	9.01
PMP2/aug-cc-pVDZ	8.98	8.78
ROMP2/aug-cc-pVDZ	9.07	8.87
CCSD(T)/aug-cc-pVDZ	8.82	8.65
CASSCF	8.15	7.76
CASPT2	8.66	8.43
MRCI	8.59	8.49

atom is 1.84 Å, and that with the hydrogen atom amounts to 2.23 Å, while the H-bond length between the two water molecules is 1.84 Å. The optimized cationic structure for the two-water cluster, where water molecules interact with two hydrogens in imidazole cation, is presented in Figure 2f.

For the neutral imidazole$(H_2O)_3$ cluster, two equivalent global minima were found (Figure 3a,b), which are mirror images of each other. Water molecules continue to form H-bonds between themselves, which results in a bent water chain either above or below the imidazole molecule. The H-bond distance between the nitrogen and hydrogen atoms for both of the lowest structures is 1.87 Å, the H-bond length with oxygen is 2.04 Å, and the O−H distances between water molecules are 1.80 Å and 1.82 Å. We also identified low lying minima (with energy higher up to 2 kcal/mol above the global minimum) with a water chain either placed perpendicular to the plane of the imidazole molecule or parallel to it.

The neutral imidazole$(H_2O)_4$ cluster looks similar to clusters with 2−3 water molecules, i.e., water molecules form a solvation ring both aside and above imidazole (Figure 3c−f). We identified four low lying minima, three of them having almost the same geometry, differing only in hydrogen ordering within the chain of water molecules. However, the geometry of the fourth minimum is very different from the others, since, in this case, the water ring is oriented almost perpendicularly to the imidazole plane. Finally, in the case of $n = 5$ (Figure 3g) water molecules in the lowest minimum form a bent chain, where two water molecules are not directly bound to imidazole, but are rather located in a second solvation shell, forming H-bonds only with other water molecules.

The calculated VIPs of neutral imidazole$(H_2O)_n$ for $n = 1-5$ and AIP for clusters with one to two water molecules obtained at the PMP2/aug-cc-pvdz level of theory are presented in Table 4. Also, VIP for $n = 1-3$ clusters calculated at the CCSD(T)/aug-cc-pvdz level and for an $n = 1$ cluster calculated employing CASPT2, MRCI are shown. For these clusters, the VIP values calculated at the PMP2 level are very close to the CCSD(T) values, the former being overestimated by only 0.2 eV. Also, similarly to isolated imidazole, even for the imidazole−water complexes, the multireference effects do not significantly affect the overall picture (see Table 4). The changes induced by the complexation are approximately the same at CASPT2, MRCI, and PMP2 levels. Note that, even for the largest investigated cluster, VIP remains significantly above the experimental bulk value, which is due to the lack of long range solvent polarization in the cluster system (see below).

The adiabatic ionization potential shifts considerably more than the vertical one upon the addition of the first water molecule. This rather high difference between VIP and AIP is related to the fact that, for the ionized imidazole, the first water molecule binds to a completely different site (with a N···O binding motive, see Figure 2e) than for the neutral molecule (with a O−H···N bond, Figure 2b). This difference demonstrates for a cluster system the effect of the nuclear part of solvent polarization.

3.3. Point Charges Model of the Solvent. Vertical ionization potential values obtained using bulk classical or ab initio MD simulations are listed in Table 5. VIP values calculated for this system with all water molecules in the unit cell represented as SPC point charges, for geometry taken either from classical or

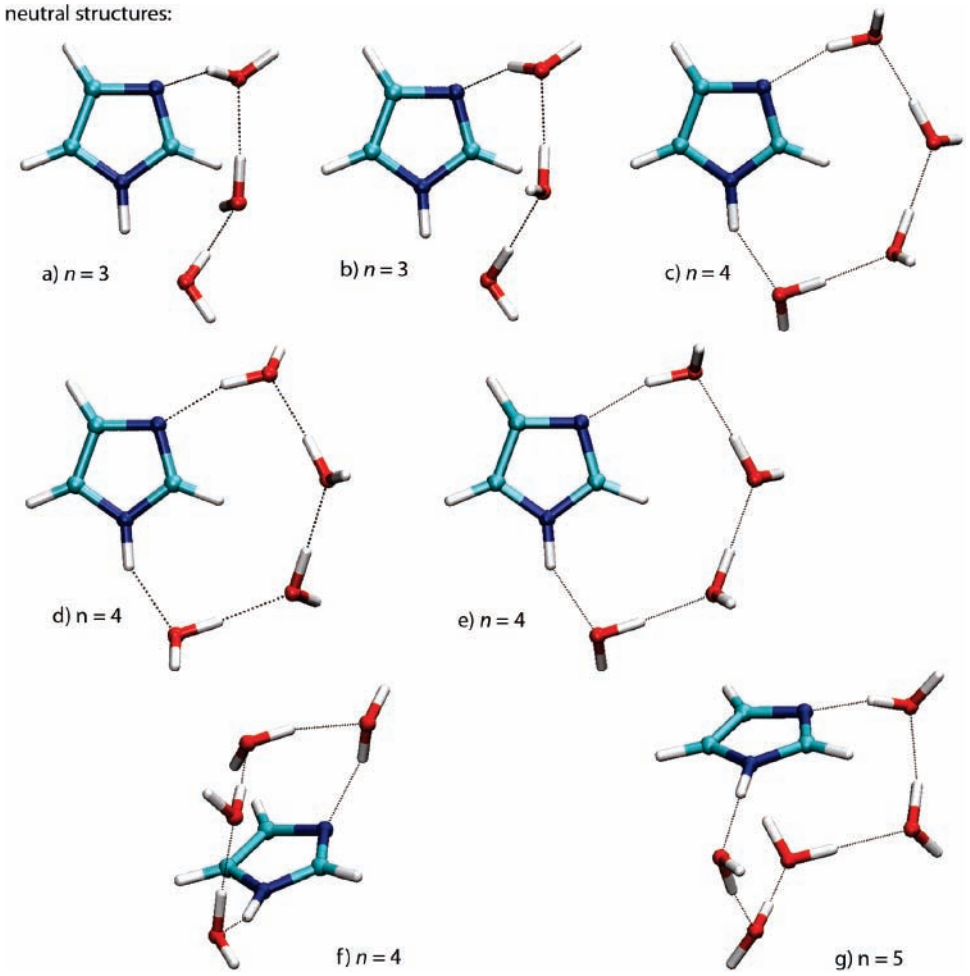

Figure 3. Structures of neutral imidazole$(H_2O)_n$ clusters for $n = 3-5$.

TABLE 4: Calculated Adiabatic (AIP) and Vertical (VIP) Ionization Potentials (in eV) of Imidazole$(H_2O)_n$ ($n = 1-5$) at the PMP2/aug-cc-pvDZ and CCSD(T)/ aug-cc-pvDZ Levels of Theory

n H_2O	VIP_PMP2 [eV]	VIP_CCSD(T) [eV]	AIP_PMP2 [eV]	CASPT2 (VIP/AIP)	MRCI (VIP/AIP)
1	9.26	9.10	8.29	8.93/7.99	8.84/7.92
2	9.14	8.99	8.31		
3	8.83	8.66			
4	8.78				
5	9.08				

TABLE 5: Vertical (VIP) Ionization Potential (in eV) of Neutral Imidazole in Water Calculated Using Water Charge Distributions from MD Simulation

molecular dynamics method/potential	charges	VIP [eV]
classical, SPC	SPC	9.50
classical SPC	ab initio + SPC	9.45
ab initio	SPC	9.62
ab initio	ab initio + SPC	9.53

ab initio MD, are around 9.5 eV. A more sophisticated approach with water molecules in the first solvation shell treated explicitly in electronic structure calculations changes the results only slightly (VIP is lowered by about 0.1 eV). Interestingly, these results are not in better agreement with experimental VIP than those presented above for cluster microsolvation. This is likely due to the neglect of electronic polarization of the solvent during the ionization process (*vide infra*).

3.4. Continuum Models. For the vertical ionization potential, only the fast component of polarization was included in the polarizable continuum calculations (nonequilibrium PCM), while for the adiabatic ionization potential both the fast and slow components of the polarization were considered (equilibrium PCM). Bare neutral imidazole embedded in the polarizable continuum exhibits a VIP of 7.87 eV. This value is more than 1 eV lower than both the VIPs and AIPs of imidazole in the gas phase or even in the microhydrated environment, and it is significantly closer to the result of the photoelectron experiment. This difference reflects the electronic part of the water polarization. The AIP of 6.45 eV is significantly smaller than the VIP and actually lies below the onset of the PE peak (Figure 1) implying a vanishing Franck−Condon overlap between the initial and final states. Most of the difference between calculated VIPs and AIPs can be attributed to the long-range nuclear polarization of the water solvent.

3.5. Hybrid Models. In order to account for both specific solvation and long-range effects on the ionization potentials, we have also employed a combined model, in which neutral imidazole$(H_2O)_n$ clusters, $n = 1-5$, are embedded into the aqueous polarizable continuum. Results of these calculations are summarized in Table 6. The addition of explicit water molecules has only a small effect on the ionization potential values. Within PCM, the vertical ionization potentials slightly increase, from 7.87 eV for the bare neutral imidazole to 8.06 eV for neutral imidazole with five explicit water molecules. Note that this number is already very close to the experimental value of 8.26 eV.

TABLE 6: Vertical (VIP) Ionization Potential (in eV) of Imidazole in Water Calculated Using a Nonequilibrium Polarizable Continuum Solvent Model at the PMP2/aug-cc-pvDZ Level of Theory[a]

n H_2O	VIP [eV]
0	7.87
1	7.96
2	7.97
3(a)	7.93
3(b)	7.93
4(c)	7.95
4(d)	7.95
4(e)	7.95
4(f)	8.06
5	8.06

[a] The notation of isomers is the same as in Figure 3.

4. Discussion and Conclusions

From the present computational and experimental study, the following conclusions concerning the ionization potential of neutral imidazole in water can be drawn. First, inclusion of the long-range polarization of the water solvent by the solute is important. This effect cannot be recovered only by microsolvating the investigated species by a small number of water molecules, and the solvent effects beyond the first solvent shell have to be included. Employing a point charge water model for geometries from bulk MD simulations still does not accurately reproduce the experimental energies since the electronic part of the solvent polarization effect during the ionization process is missing. Second, for reproducing the experimental vertical ionization energy of aqueous neutral imidazole within a couple tenths of an electronvolt, the nonequilibrium polarizable continuum approach for recovering long-range polarization performs very well. However, care has to be taken to include only the fast electronic (and not the slow nuclear) component of solvent relaxation when comparing to the measured *vertical* ionization energy. This is different from the *adiabatic* ionization energy, which accounts also for nuclear rearrangements within the solute and the solvent upon ionization. While this change is small for the imidazole solute, the rearrangement of the nearest water molecules, as well as longer range water reorientations upon ionization of imidazole are sizable.

Acknowledgment. We are grateful to the anonymous reviewer for valuable comments, particularly concerning benchmarking of the new method. We thank the Czech Ministry of Education (Grant LC512) and the Grant Agency of the Czech Republic (Grant 203/07/1006 to P.J.) for support. P.S. acknowledges a postdoctoral grant from the Grant Agency of the Czech Republic, 203/07/P449.

References and Notes

(1) Wishart, J. F.; Castner, E. W. *J. Phys. Chem. B* **2007**, *111*, 4639.
(2) Winter, B.; Faubel, M. *Chem. Rev.* **2006**, *106*, 1176.
(3) Miertus, S.; Scrocco, E.; Tomasi, J. *Chem. Phys.* **1981**, *55*, 117.
(4) Tomasi, J.; Mennuci, B.; Cammi, R. *Chem. Rev.* **2005**, *105*, 2999.
(5) Mennucci, B. *Theor. Chem. Acc.* **2006**, *116*, 31.
(6) Marcus, R. A. *J. Chem. Phys.* **1963**, *39*, 1734.
(7) Mennucci, B.; Cammi, R.; Tomasi, J. *J. Chem. Phys.* **1998**, *109*, 2798.
(8) Cossi, M.; Barone, V. *J. Phys. Chem. A* **2000**, *104*, 10614.
(9) Cossi, M.; Barone, V. *J. Chem. Phys.* **2000**, *112*, 2427.
(10) Caricato, M.; Ingrosso, F.; Mennucci, B.; Tomasi, J. *J. Chem. Phys.* **205**, *122*, 154501.
(11) Weber, R.; Winter, B.; Schmidt, P. M.; Widdra, W.; Hertel, I. V.; Dittmar, M.; Faubel, M. *J. Phys. Chem. B* **2004**, *108*, 4729.
(12) Schlegel, H. B. *J. Chem. Phys.* **1986**, *84*, 4530.
(13) Crespo-Hernandez, C. E.; Arce, R.; Ishikawa, Y.; Gorb, L.; Leszczynski, J.; Close, D. M. *J. Phys. Chem. A* **2004**, *108*, 6373.
(14) VandeVondele, J; Krack, M.; Mohamed, F.; Parrinello, M.; Chassaing, T.; Hutter, *J. Comput. Phys. Commun.* **2005**, *167*, 103.
(15) Case, D. A.; Darden, T. A.; Cheatham, T. E., III; Simmerling, C. L.; Wang, J.; Duke, R. E.; Luo, R.; Merz, K. M.; Wang, B.; Pearlman, D. A.; Crowley, M.; Brozell, S.; Tsui, V.; Gohlke, H.; Mongan, J.; Hornak, V.; Cui, G.; Beroza, P.; Schafmeister, C.; Caldwell, J. W.; Ross, W. S.; Kollman P. A. *Amber 8*; University of California: San Francisco, CA, 2004.
(16) Wang, J.; Wang, W.; Kollman, P. A.; Case, D. A. *J. Mol. Graphics Modell.* **2006**, *25*, 247.
(17) Wang, J.; Wolf, R. M.; Caldwell, J. W.; Kollman, P. A.; Case, D. A. *J. Comput. Chem.* **2004**, *25*, 1157.
(18) Frisch, M. J.; Trucks, G. W.; Schlegel, H. B.; Scuseria, G. E.; Robb, M. A.; Cheeseman, J. R.; Montgomery, J. A., Jr.; Vreven, T.; Kudin, K. N.; Burant, J. C.; Millam, J. M.; Iyengar, S. S.; Tomasi, J.; Barone, V.; Mennucci, B.; Cossi, M.; Scalmani, G.; Rega, N.; Petersson, G. A.; Nakatsuji, H.; Hada, M.; Ehara, M.; Toyota, K.; Fukuda, R.; Hasegawa, J.; Ishida, M.; Nakajima, T.; Honda, Y.; Kitao, O.; Nakai, H.; Klene, M.; Li, X.; Knox, J. E.; Hratchian, H. P.; Cross, J. B.; Bakken, V.; Adamo, C.; Jaramillo, J.; Gomperts, R.; Stratmann, R. E.; Yazyev, O.; Austin, A. J.; Cammi, R.; Pomelli, C.; Ochterski, J. W.; Ayala, P. Y.; Morokuma, K.; Voth, G. A.; Salvador, P.; Dannenberg, J. J.; Zakrzewski, V. G.; Dapprich, S.; Daniels, A. D.; Strain, M. C.; Farkas, O.; Malick, D. K.; Rabuck, A. D.; Raghavachari, K.; Foresman, J. B.; Ortiz, J. V.; Cui, Q.; Baboul, A. G.; Clifford, S.; Cioslowski, J.; Stefanov, B. B.; Liu, G.; Liashenko, A.; Piskorz, P.; Komaromi, I.; Martin, R. L.; Fox, D. J.; Keith, T.; Al-Laham, M. A.; Peng, C. Y.; Nanayakkara, A.; Challacombe, M.; Gill, P. M. W.; Johnson, B.; Chen, W.; Wong, M. W.; Gonzalez, C.; and Pople, J. A. *Gaussian 03*, revision C.02; Gaussian, Inc.: Wallingford, CT, 2004.
(19) Lide, D. R. *Handbook of Chemistry and Physics*; CRC Press: Boca Raton, FL, 1997.
(20) Winter, B.; Weber, R.; Hertel, I. V.; Faubel, M.; Jungwirth, P.; Brown, E. C.; Bradforth, S. E. *J. Am. Chem. Soc.* **2005**, *127*, 7203.
(21) Winter, B.; Faubel, M.; Hertel, I. V.; Pettenkofer, C.; Bradforth, S. E.; Jagoda-Cwiklik, B.; Cwiklik, L.; Jungwirth, P. *J. Am. Chem. Soc.* **2006**, *128*, 3864.
(22) Werner, H.-J.; Knowles, P. J.; Lindh, R.; Manby, F. R.; Schütz, M.; Celani, P.; Korona, T.; Rauhut, G.; Amos, R. D.; Bernhardsson, A.; Berning, A.; Cooper, D. L.; Deegan, M. J. O.; Dobbyn, A. J.; Eckert, F.; Hampel, C.; Hetzer, G.; Lloyd, A. W.; McNicholas, S. J.; Meyer, W.; Mura, M. E.; Nicklass, A.; Palmieri, P.; Pitzer, R.; Schumann, U.; Stoll, H.; Stone, A. J.; Tarroni, R.; Thorsteinsson, T. *MOLPRO*, version 2006.1. http://www.molpro.net.
(23) Winter, B.; Weber, R.; Widdra, W.; Dittmar, M.; Faubel, M.; Hertel, I. V. *J. Phys. Chem. A* **2004**, *108*, 2625.
(24) Machado, F. B. C.; Davidson, E. R. *J. Chem. Phys.* **1992**, *97*, 1881.
(25) Orlov, V. M.; Smirnovv, A. N.; Varshavsky, Y. M. *Tetrahedron Lett.* **1976**, *48*, 4377.
(26) Roca-Sanjuan, D.; Rubio, M.; Merchan, M.; Serrano-Andres, L. *J. Chem. Phys.* **2006**, *125*, 084302.